

Unparticle physics with broken scale invariance

Vernon Barger^a, Yu Gao^a, Wai-Yee Keung^b, Danny Marfatia^c and V. Nefer Şenoğuz^c

^a*Department of Physics, University of Wisconsin, Madison, WI 53706, USA*

^b*Department of Physics, University of Illinois, Chicago, IL 60607-7059, USA*

^c*Department of Physics and Astronomy, University of Kansas, Lawrence, KS 66045, USA*

E-mail: barger@pheno.wisc.edu, yugao@physics.wisc.edu, keung@uic.edu, marfatia@ku.edu, nefer@ku.edu

ABSTRACT: If scale invariance is exact, unparticles are unlikely to be probed in colliders since there are stringent constraints from astrophysics and cosmology. However these constraints are inapplicable if scale invariance is broken at a scale $\mu \gtrsim 1$ GeV. The case $1 \text{ GeV} \lesssim \mu < M_Z$ is particularly interesting since it allows unparticles to be probed at and below the Z pole. We show that μ can naturally be in this range if only vector unparticles exist, and briefly remark on implications for Higgs phenomenology. We then obtain constraints on unparticle parameters from $e^+e^- \rightarrow \mu^+\mu^-$ cross-section and forward-backward asymmetry data, and compare with the constraints from mono-photon production and the Z hadronic width.

1. Introduction

Unparticle physics was introduced in Ref. [1] as a low energy effective description of a hidden sector with a nontrivial infrared fixed point. This sector is assumed to interact with the Standard Model (SM) through the exchange of particles at a high scale M . Below M , the interactions are of the form

$$\frac{C_i}{M^{d_{UV}+d_{SM}^i-4}} O_{SM}^i O_{UV}, \quad (1.1)$$

where C_i are dimensionless constants, O_{SM}^i is an operator with mass dimension d_{SM}^i built out of SM fields and O_{UV} is an operator with mass dimension d_{UV} built out of the hidden sector fields. Scale invariance in the hidden sector emerges at an energy scale $\Lambda < M$. In the effective theory below Λ the interactions of Eq. (1.1) take the form

$$\frac{C_i \Lambda^{d_{UV}-d}}{M^{d_{UV}+d_{SM}^i-4}} O_{SM}^i O, \quad (1.2)$$

where d is the scaling dimension of the unparticle operator O .

Unparticle effects might be detectable in missing energy distributions and interference with SM amplitudes [1, 2, 3, 4]. However, if scale invariance is exact, unparticles are unlikely to be probed in colliders since there are strong constraints from astrophysics and cosmology [5, 6] (see Section 2). As discussed in Section 3, these constraints are inapplicable if scale invariance is broken at a scale $\mu \gtrsim 1$ GeV, while constraints from experiments at center-of-mass energy $\sqrt{s} > \mu$ remain relevant and resonance-like behavior at μ is expected. Ref. [7] has considered collider phenomenology for $\mu > M_Z$. Here we consider the constraints on unparticle parameters assuming $1 \text{ GeV} \lesssim \mu < M_Z$ which allows unparticles to be probed by s channel Z exchange observables.

For scales of Λ and M that are experimentally accessible, the Higgs coupling to scalar unparticles generally breaks scale invariance at the electroweak scale [8, 9]. Having $\mu < M_Z$ in this case requires somewhat small dimensionless couplings (Section 3.1). However, if only vector unparticles exist, scale invariance is broken by higher dimensional operators, and μ can naturally be below M_Z (Section 3.2). We also briefly discuss how vector unparticles could affect Higgs phenomenology in Section 3.3.

Constraints on vector and axial-vector unparticle couplings obtained using $e^+e^- \rightarrow \mu^+\mu^-$ forward-backward asymmetry (FBA) and total cross-section data are presented in Section 4. The resonance-like behaviour at μ is taken into account in the analysis. Our summary is followed by four appendices covering details of the unparticle contribution to the Z hadronic width, the bound from SN 1987A cooling, the vacuum polarization correction to the unparticle propagator, and the initial state QED corrections.

2. Bounds on vector unparticle interactions

Consider vector unparticles coupling to fermions:

$$\mathcal{L}_\psi = C_V \frac{\Lambda^{d_{UV}-d}}{M^{d_{UV}-1}} \bar{\psi} \gamma_\mu \psi O^\mu + C_A \frac{\Lambda^{d_{UV}-d}}{M^{d_{UV}-1}} \bar{\psi} \gamma_\mu \gamma_5 \psi O^\mu, \quad (2.1)$$

which, following the convention of Refs. [2, 10], can be written as

$$\frac{c_V}{M_Z^{d-1}} \bar{\psi} \gamma_\mu \psi O^\mu + \frac{c_A}{M_Z^{d-1}} \bar{\psi} \gamma_\mu \gamma_5 \psi O^\mu, \quad (2.2)$$

with

$$c_{V,A} = C_{V,A} \left(\frac{\Lambda}{M} \right)^{d_{UV}-1} \left(\frac{M_Z}{\Lambda} \right)^{d-1}. \quad (2.3)$$

Using the spectral density $\rho(m^2) = A_d(m^2)^{d-2}$ [1], the propagator is [2, 3, 4]

$$[\Delta_F(q^2)]_{\mu\nu} = \frac{A_d}{2 \sin(d\pi)} (-q^2)^{d-2} \left(-g_{\mu\nu} + a \frac{q_\mu q_\nu}{q^2} \right). \quad (2.4)$$

Here $(-q^2)^{d-2}$ is defined as $|q^2|^{d-2}$ for negative q^2 and $|q^2|^{d-2} e^{-id\pi}$ for positive q^2 . A_d is chosen following the convention of Ref. [1]:

$$A_d = \frac{16\pi^{5/2} \Gamma(d+1/2)}{(2\pi)^{2d} \Gamma(d-1) \Gamma(2d)}. \quad (2.5)$$

The constant $a = 1$ if O^μ is assumed to be transverse, and $a = 2(d-2)/(d-1)$ in conformal field theories [11]. The value of a does not affect the results of this paper.

It should be noted that operators of a conformal field theory are subject to lower bounds on their scaling dimensions from unitarity, and in particular $d \geq 3$ for vector operators [11, 12]. However, this bound can be violated for a hypothetical scale invariant field theory that is not conformally invariant (see e.g. Ref. [13]). We focus on the range $1 < d < 2$ since unparticle effects are relatively suppressed for higher values of d . (Also, SM contact interactions induced by messenger exchange at the scale M generally dominate over unparticle interference effects for $d \geq 3$ [11].)

A bound on the scale of O^μ interactions can be obtained from mono-photon production ($e^+e^- \rightarrow \gamma + \text{unparticle}$) at LEP2. The cross-section is given by [3]

$$d\sigma = \frac{A_d e^2 c^2}{8\pi^3 M_Z^2 E_\gamma s} \left(\frac{s - 2\sqrt{s} E_\gamma}{M_Z^2} \right)^{d-2} \frac{s - 2\sqrt{s} E_\gamma + (1 + \cos^2 \theta_\gamma) E_\gamma^2}{1 - \cos^2 \theta_\gamma} dE_\gamma d\Omega, \quad (2.6)$$

where $c \equiv \sqrt{c_V^2 + c_A^2}$, E_γ is the photon energy, and θ_γ is the polar angle. Following Ref. [4], we obtain an upper bound on c using the L3 95% C.L. upper limit $\sigma \simeq 0.2$ pb (obtained under the cuts $E_\gamma > 5$ GeV and $|\cos \theta_\gamma| < 0.97$ at $\sqrt{s} = 207$ GeV) [14]. This ‘‘mono-photon bound’’ corresponds to $c < 0.026$, 0.032 and 0.057 for $d = 1.1$, 1.5 and 1.9 respectively. Note that since $\Lambda < M$ and unparticle effects can only be probed if $\sqrt{s} < \Lambda$, $c \gtrsim (M_Z/\sqrt{s})^{d-1}$ is theoretically inaccessible. This implies that the current bound from mono-photon production is only relevant for $d \lesssim 2.6$ (see Fig. 1).¹

Another process considered in Ref. [3] is $Z \rightarrow q\bar{q} + \text{unparticle}$, which contributes to the Z hadronic width. Here we note that it is important to consider the vertex correction

¹Mono- Z production is also considered in Refs. [4, 15]. Similarly to mono-photon production, upper bounds on c can be obtained using the L3 limit on Z +missing energy cross-section [16], but they are weaker than the mono-photon bounds.

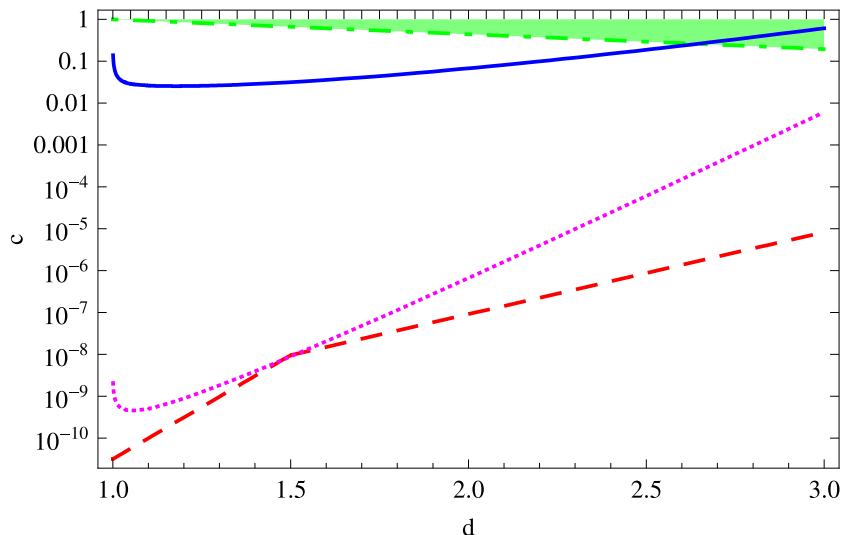


Figure 1: Upper bounds on c from mono-photon production (solid blue curve), BBN (dashed red curve) and SN 1987A (dotted magenta curve). The shaded region corresponds to the theoretically forbidden region $c > (M_Z/\sqrt{s})^{d-1}$.

together with the real emission process, since the two contributions largely cancel each other for values of d close to 1 and the former contribution dominates for values of d close to 2. As explained in Appendix A, the constraint on unparticles from the Z hadronic width is also weaker than the mono-photon bound.

We now compare the mono-photon bound with the constraints on vector unparticles from cosmology and astrophysics [5]. To preserve the successful predictions of Big Bang Nucleosynthesis (BBN), we require the unparticle sector to be colder than SM radiation during BBN, so that its energy density is subdominant. For the operator in Eq. (2.2), the interaction rate Γ_ψ redshifts more slowly than the Hubble parameter \mathcal{H} if $d \leq 3/2$. The unparticle sector can then remain cold if it is decoupled throughout BBN, corresponding to $\Gamma_\psi \lesssim \mathcal{H}$ for $T \sim 1$ MeV. For $d > 3/2$, Γ_ψ redshifts faster than \mathcal{H} . In this case we require the unparticle sector to decouple before $T \sim 1$ GeV so that the QCD phase-transition only heats up SM radiation [5]. The BBN constraint, corresponding to

$$\left(\frac{c}{M_Z^{d-1}}\right)^2 \lesssim \frac{T^{3-2d}}{10^{18} \text{ GeV}} \begin{cases} T \sim 1 \text{ MeV} & \text{if } d \leq 3/2 \\ T \sim 1 \text{ GeV} & \text{if } d > 3/2 \end{cases}, \quad (2.7)$$

is much more stringent than the mono-photon bound (see Fig. 1). The SN 1987A constraint on unparticle emission [5, 6, 17, 18],

$$C_d \left(\frac{c}{M_Z^{d-1}}\right)^2 \lesssim 4 \cdot 10^{-22} T_{SN}^{2-2d}, \quad (2.8)$$

where the supernova core temperature is taken to be $T_{SN} = 30$ MeV and $C_d \simeq 0.01$ (see Appendix B), is similar in magnitude to the BBN constraint.

3. Broken scale invariance

The BBN and SN 1987A constraints can be evaded provided scale invariance is broken at a scale μ sufficiently large compared to the relevant energy scales ($\simeq 1$ MeV and $\simeq T_{SN}$ respectively).² We can model broken scale invariance by removing modes with energy less than μ in the spectral density, so that [8]

$$\rho(m^2) = A_d \theta(m^2 - \mu^2) (m^2 - \mu^2)^{d-2}, \quad (3.1)$$

$$[\Delta_F(q^2)]_{\mu\nu} = \frac{A_d}{2 \sin(d\pi)} [-(q^2 - \mu^2)]^{d-2} \left(-g_{\mu\nu} + a \frac{q_\mu q_\nu}{q^2} \right), \quad (3.2)$$

where $[-(q^2 - \mu^2)]^{d-2}$ is defined as $|q^2 - \mu^2|^{d-2}$ for $q^2 < \mu^2$ and $|q^2 - \mu^2|^{d-2} e^{-id\pi}$ for $q^2 > \mu^2$.

Due to Boltzmann suppression of the emission, the SN 1987A constraint with scale invariance broken at a scale μ corresponds to replacing C_d in Eq. (2.8) by (see Appendix B):

$$C_d \approx \frac{A_d}{2^{(9/2)-d} \pi^{7/2} (d-1)^{2-d}} \left(\frac{\mu}{T_{SN}} \right)^{d+5/2} e^{-\mu/T_{SN}}. \quad (3.3)$$

Assuming c is close to the mono-photon bound, the SN 1987A constraint can be evaded provided $\mu \gtrsim 1$ GeV. Note that other constraints arising from long range forces [20], contributions to the muon and electron anomalous magnetic moments [3, 21], modifications to positronium decay [21], neutrino decay into unparticles [22], and contributions to low energy neutrino-electron scattering amplitudes [23] are also evaded in this case.

The mono-photon bound is also modified when scale invariance is broken: In Eq. (2.6), the numerator inside the parentheses is replaced by $s - 2\sqrt{s}E_\gamma - \mu^2$, and the end-point for E_γ is shifted from $\sqrt{s}/2$ to $(s - \mu^2)/2\sqrt{s}$. However, these modifications do not change the cross-section appreciably for $\mu < M_Z$.

Whether scale invariance is broken or not is relevant for the allowed range of the vector unparticle scale dimension d . Consider the decay width from the interaction Eq.(2.2) where an initial fermion with mass m_f decays into a massless fermion and the unparticle. Following Ref. [24], we obtain

$$\frac{d\Gamma}{dE} = \frac{A_d c^2}{4\pi^2 M_Z^{2d-2}} \frac{E^2 [(2+a)m_f^2 - 4m_f E]}{(m_f^2 - 2m_f E)^{3-d}} \theta(m_f - 2E), \quad (3.4)$$

where E is the energy of the final fermion. Integrating over dE , it follows that the total decay width diverges for $d < 2$. This is due to the extra $(1/q^2)$ factor associated with the vector propagator. However, once scale invariance is broken, values of $q^2 < \mu^2$ are removed from the phase space:

$$\frac{d\Gamma}{dE} = \frac{A_d c^2}{4\pi^2 M_Z^{2d-2}} \frac{E^2 [(2+a)m_f^2 - 4m_f E]}{(m_f^2 - 2m_f E)(m_f^2 - 2m_f E - \mu^2)^{2-d}} \theta(m_f^2 - 2m_f E - \mu^2), \quad (3.5)$$

²Although unparticles are stable if scale invariance is exact, it is not clear if they remain so when scale invariance is broken. If they are stable, and if μ is less than the top quark mass, it is not sufficient that they decouple at ~ 1 GeV for $d > 3/2$. Instead, they should remain out of equilibrium at all temperatures before BBN, at least up to the reheating temperature [19].

and the total width remains finite and positive for $d < 2$.³

Next, we discuss how scale invariance could be broken such that $1 \text{ GeV} \lesssim \mu < M_Z$, first considering the influence of scalar unparticles and then assuming only vector unparticles couple to the SM.

3.1 Scalar unparticles

As pointed out in Ref. [8], scale invariance is broken by the operator

$$C_2 \frac{\Lambda^{d_{UV}-d}}{M^{d_{UV}-2}} H^\dagger H O, \quad (3.6)$$

where H is the SM Higgs doublet, at an energy scale

$$\mu \simeq \left[C_2 v^2 \left(\frac{\Lambda}{M} \right)^{d_{UV}-2} \Lambda^{2-d} \right]^{1/(4-d)}, \quad (3.7)$$

where $v = 174 \text{ GeV}$. Having an experimentally accessible conformal window $\mu \ll \Lambda \sim v$ requires $C_2 \ll 1$ [9]. Assuming $\mu < M_Z$, another upper bound on μ and C_2 can be obtained from the threshold correction to the fine structure constant [9]. If the operator

$$C_4 \frac{\Lambda^{d_{UV}-d}}{M^{d_{UV}}} F^{\rho\delta} F_{\rho\delta} O \quad (3.8)$$

exists, the value of $\alpha^{-1}(M_Z)$ remains within the current uncertainty for

$$\mu \lesssim \left(\frac{M}{\Lambda} \right)^{d_{UV}/d} \left(\frac{1}{10^{4.5} C_4} \right)^{1/d} \Lambda. \quad (3.9)$$

Eq. (3.9) provides an upper bound on μ , whereas Eqs. (2.8, 3.3) provide a lower bound. There can be a scale invariant window below M_Z between these two bounds without violating any of the other constraints discussed above. As a specific example we take $d_{UV} = 2$ or 3 , $C_V = C_A = 1$ and $\Lambda = v$. Setting M equal to the mono-photon bound using Eqs. (2.3, 2.6), we calculate the range of C_2 , C_4 and μ that satisfies the other constraints. As shown in Table 1 and Fig. 2, there is an allowed range of μ below M_Z , provided the scalar unparticle operators couple somewhat weakly ($C_4, C_2 \lesssim 0.1$) compared to vector operators ($C_V = C_A = 1$).

3.2 Vector unparticles

Even if only vector unparticles exist, scale invariance can still be broken if the Higgs couples to higher-dimensional operators such as $O^\mu O_\mu$. Furthermore, due to the higher dimensionality, the scale μ is naturally suppressed compared to the electroweak scale.⁴ Consider the operators

$$\frac{\Lambda^{2d_{UV}-d_*}}{M^{2d_{UV}-2}} H^\dagger H O^\mu O_\mu + \frac{\Lambda^{2d_{UV}-d_*}}{M^{2d_{UV}}} F^{\rho\delta} F_{\rho\delta} O^\mu O_\mu \quad (3.10)$$

³For scalar unparticles and $d < 1$, the divergence pointed out in Ref. [1] remains whether $\mu = 0$ or not.

⁴See Ref. [25] for a similar scenario with charged scalar unparticles.

| $d_{UV} = 2$ | | | $d_{UV} = 3$ | | | |
|--------------|-----------|-------------|-------------------------|-----------|-------------|-------------------------|
| d | M (GeV) | μ (GeV) | C_2 | M (GeV) | μ (GeV) | C_2 |
| 1.1 | 8800 | $1.5-M_Z$ | $9 \times 10^{-7}-0.15$ | 1200 | $1.5-35$ | $7 \times 10^{-6}-0.07$ |
| 1.5 | 5600 | $1.3-74$ | $4 \times 10^{-6}-0.12$ | 990 | $1.3-31$ | $2 \times 10^{-5}-0.08$ |
| 1.9 | 2400 | $1.1-49$ | $2 \times 10^{-5}-0.07$ | 650 | $1.1-25$ | $8 \times 10^{-5}-0.06$ |

Table 1: The allowed range of μ (below M_Z) and C_2 for M at the mono-photon bound, assuming $C_V = C_A = 1$ (see Eq. (2.1)), $\Lambda = v$ and $C_4 = C_2$ (see Eqs. (3.6, 3.8)).

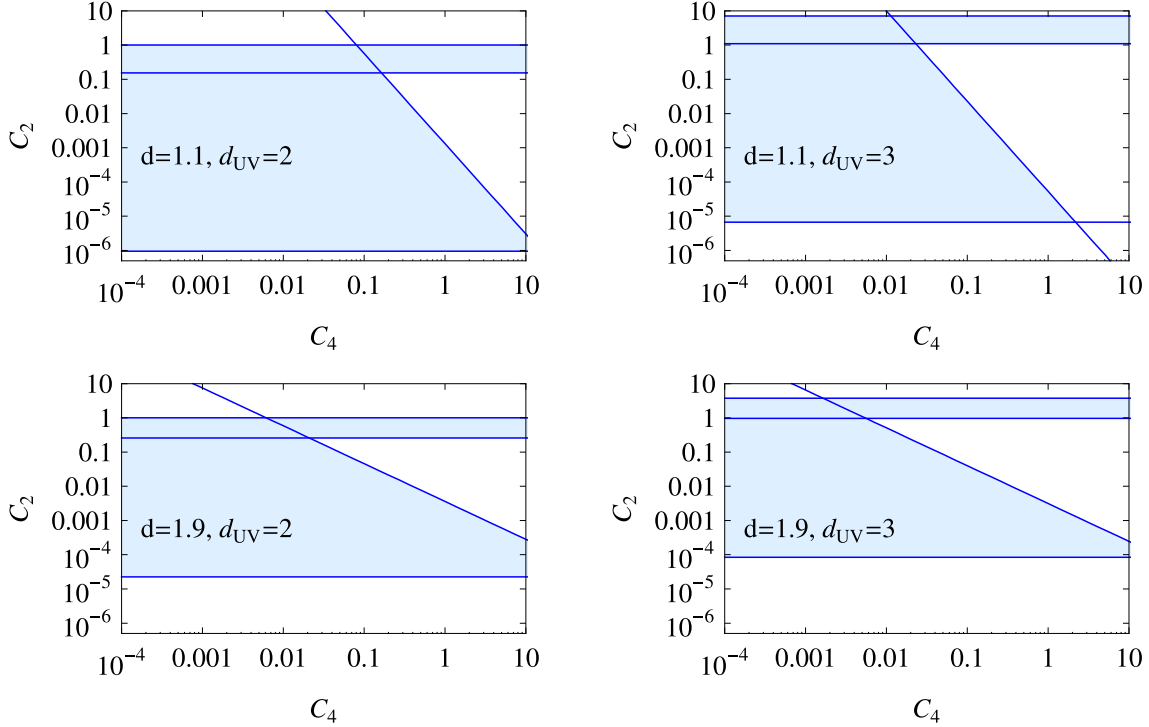


Figure 2: The shaded region in the C_4 - C_2 plane is allowed for M at the mono-photon bound ($C_V = C_A = 1$, $\Lambda = v$). The lower horizontal line corresponds to the SN 1987A constraint, the middle horizontal line corresponds to $\mu = M_Z$, and the upper line to $\mu = v$. The diagonal line is the constraint from $\alpha(M_Z)$.

where we have set $C_2 = C_4 = 1$, and the scale dimension of $O^\mu O_\mu \equiv d_* \leq 2d$. Eq. (3.7) and Eq. (3.9) are modified as follows:

$$\mu \simeq \left[\left(\frac{\Lambda}{M} \right)^{2d_{UV}-2} \Lambda^{2-d_*} v^2 \right]^{1/(4-d_*)}, \quad (3.11)$$

$$\mu \lesssim \left(\frac{M}{\Lambda} \right)^{2d_{UV}/d_*} 10^{-4.5/d_*} \Lambda. \quad (3.12)$$

As shown in Fig. 3, μ can easily lie in the allowed range.

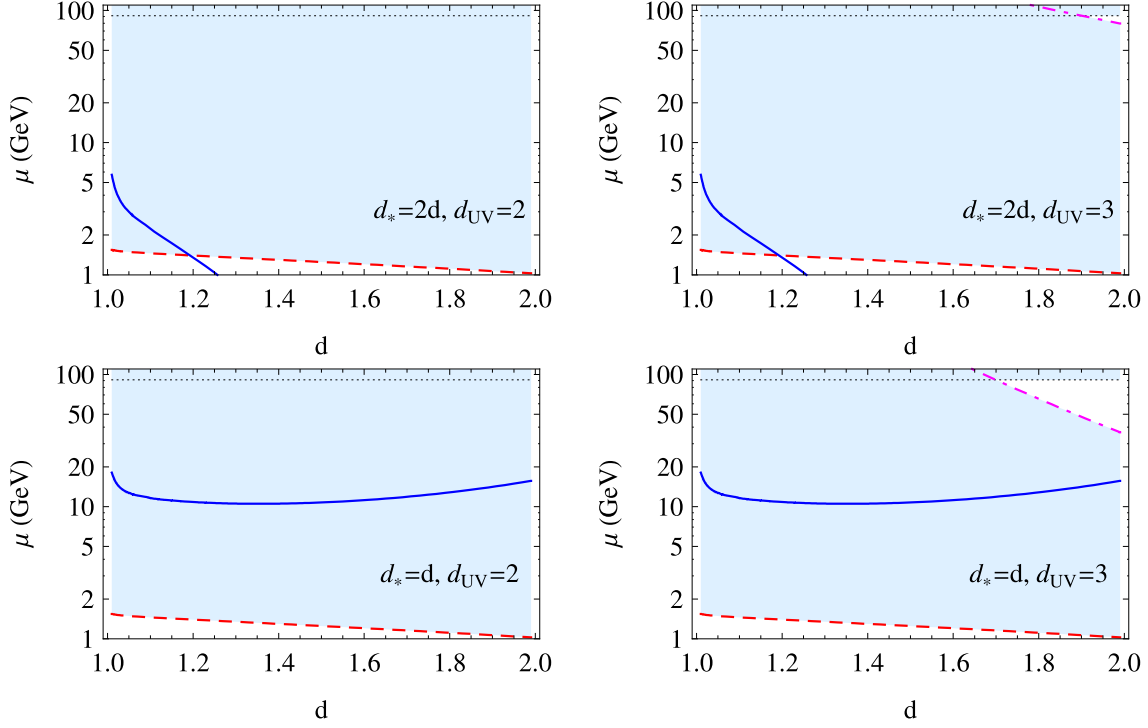


Figure 3: The shaded regions in the d - μ plane are allowed for M at the mono-photon bound ($\Lambda = v$, $C_V = C_A = 1$). The solid blue curve is μ as given by Eq. (3.11). The dashed red curve corresponds to the SN 1987A constraint, the dotted-dashed magenta curve corresponds to the constraint from $\alpha(M_Z)$, and the horizontal dotted line corresponds to $\mu = M_Z$.

3.3 Implications for Higgs phenomenology

The effects of scalar unparticles on Higgs phenomenology have been considered in Refs. [26, 27].⁵ For scalar unparticles the same operator $H^\dagger H O$ is responsible for breaking scale invariance and Higgs-unparticle mixing to lowest order, and thus the effects are suppressed for $\mu \ll M_Z$. To be more explicit, the mixing between the SM Higgs boson h and the unparticle is induced by the interaction term $(\mu^{4-d}/v) O h$. Considering the effective Higgs coupling $(1/v) C_{\gamma\gamma} h F_{\mu\nu} F^{\mu\nu}$ as an example, the contribution from the above interaction and Eq. (3.8) is given by [26]

$$C_{\gamma\gamma}(h \rightarrow O \rightarrow \gamma\gamma) \simeq C_4 \frac{e^{-id\pi} A_d}{2 \sin d\pi} \left(\frac{\mu}{m_h}\right)^{4-d} \left(\frac{m_h}{\Lambda}\right)^d \left(\frac{\Lambda}{M}\right)^{d_{UV}}. \quad (3.13)$$

Provided $\mu \ll M_Z$, this is small compared to the SM effective coupling $C_{\gamma\gamma} \sim 10^{-3}$. The Higgs partial decay width to fermions induced by the operator $\bar{\psi} \gamma_\mu D^\mu \psi O$ is similarly suppressed.

On the other hand, for vector unparticles scale invariance is broken by $H^\dagger H O^\mu O_\mu$ whereas mixing is (also) induced by

$$\frac{\Lambda^{d_{UV}-d}}{M^{d_{UV}-1}} H^\dagger D_\mu H O^\mu. \quad (3.14)$$

⁵See also Ref. [28] for supersymmetric unparticle effects.

Using Eq. (2.1) and Eq. (3.14), the effective fermionic operator is

$$\frac{1}{\Lambda_{\text{eff}}^2} H^\dagger D_\mu H \bar{\psi} \gamma^\mu \psi, \quad (3.15)$$

where

$$\frac{1}{\Lambda_{\text{eff}}^2} = \frac{1}{s} \frac{e^{-id\pi} A_d}{2 \sin d\pi} \left(\frac{\sqrt{s}}{\Lambda} \right)^{2d-2} \left(\frac{\Lambda}{M} \right)^{2(d_{UV}-1)}. \quad (3.16)$$

Contributions of this operator to Higgs production at a linear collider have been considered in Ref. [29]. The main effect is interference with the SM Higgs-strahlung (HZ) cross-section, which can be substantial in the $e^+e^- \rightarrow h\mu^+\mu^-$, $h\tau^+\tau^-$, $h\bar{q}q$ channels for M close to the mono-photon bound.

It is also interesting to note that the operator $H^\dagger H O^\mu O_\mu$ induces a partial decay width $\Gamma(h \rightarrow O^\mu O_\mu) \sim \mu^{8-2d_*}/(v^2 m_h^{5-2d_*})$. Although this is typically small, it becomes of order m_h^3/v^2 in the limit $d_* \rightarrow 4$ (i.e. $d_* \rightarrow 2d$ and $d \rightarrow 2$). With decays of $O^\mu O_\mu$ suppressed, the Higgs would then decay invisibly.

4. Muon pair production bounds on vector unparticles

We have already obtained a collider bound using Eq. (2.6). Other bounds can be obtained using the ratio $R_U \equiv \sigma(\text{with unparticles})/\sigma(\text{without unparticles})$ as well as the FBA (defined in Appendix D) for $e^+e^- \rightarrow \mu^+\mu^-$, and by combining measurements at and away from the Z pole. As shown in Ref. [2] and discussed further in Ref. [10], vector couplings of unparticles will mainly affect R_U away from the Z pole, and FBA at the Z pole. Axial-vector couplings have the opposite behaviour.

Due to the resonance-like behavior at μ (referred to as ‘‘un-resonance’’ [7]), measurements at energies around μ would be particularly sensitive to unparticle effects. Thus the bounds on $c_{V,A}$ (defined in Eq. (2.2)) for a given value of d will also depend on μ . As an example we plot FBA and R_U for $d = 1.1$ in Fig. 4. Taking $c_A = 0.026$ and $c_V = 0$, FBA = -7.2% for $\sqrt{s} = 34.8$ GeV if $\mu = 30$ GeV, to be compared with -8.3% if $\mu \ll 30$ GeV, and -8.9% for SM. Taking into account the measurement FBA = $-10.4 \pm 1.3 \pm 0.5\%$ at the same center-of-mass energy [30], it is clear that the bound on c_A for $\mu = 30$ GeV will be more stringent compared to the bound for $\mu \ll 30$ GeV (see Fig. 5).

It should be noted that for the propagator in Eq. (3.2), the area under the un-resonance diverges for $d < 1.5$. However, it is likely that once scale invariance is broken, particle-like modes will appear in the spectral density [8]. For example, vacuum polarization correction from fermion loops will modify Eq. (3.2) as follows:

$$\frac{1}{(q^2 - \mu^2)^{2-d}} \rightarrow \frac{1}{(q^2 - \mu^2)^{2-d} - \Pi(q^2)} \quad (4.1)$$

It can therefore be expected that the unparticle will become unstable, and the area under the un-resonance will depend on the decay width.

We have performed a χ^2 analysis of LEP1-Aleph, KEK-Venus and PETRA-MarkJ $e^+e^- \rightarrow \mu^+\mu^-$ cross-section and FBA data [30, 31]. The simulation includes the vacuum

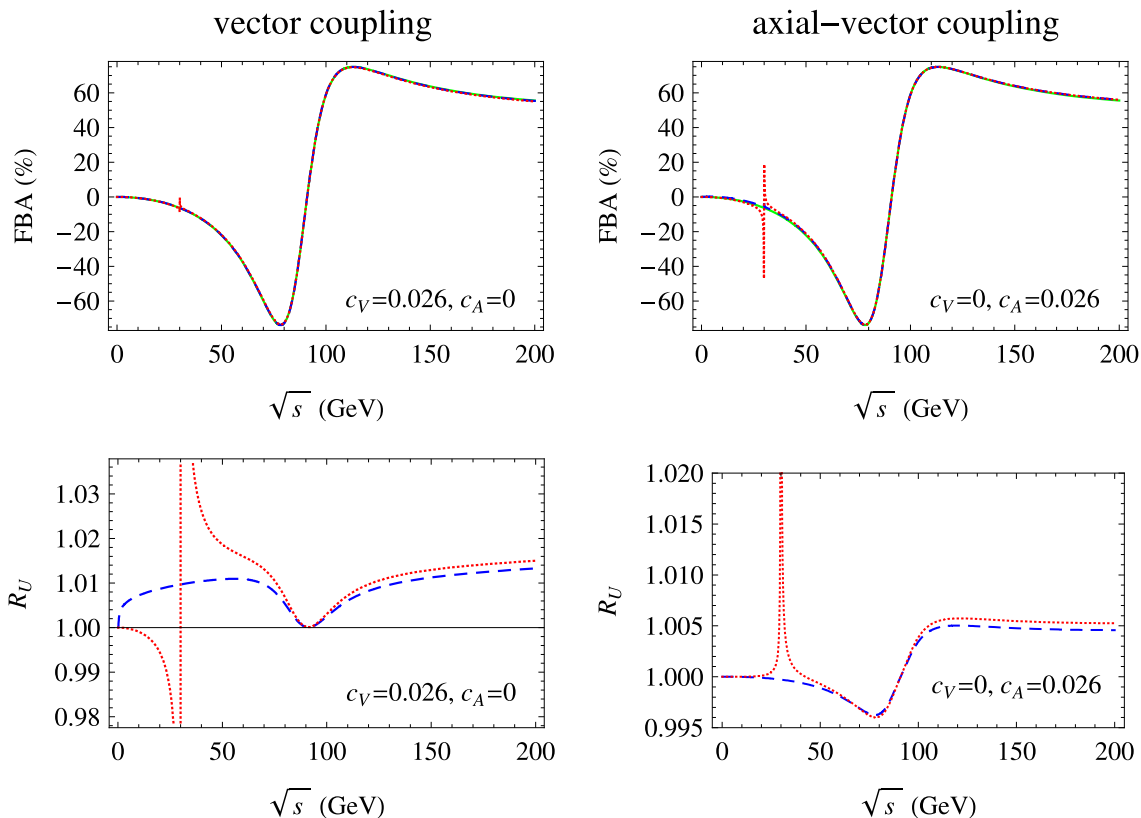


Figure 4: FBA and R_U for $e^+e^- \rightarrow \mu^+\mu^-$ with $d = 1.1$. Solid green curves: SM; dashed blue curves: unparticles with $\mu = 0$, dotted red curves: unparticles with $\mu = 30$ GeV. ($c_{V,A} = 0.026$ correspond to the mono-photon bound of section 2.)

polarization correction from fermion loops to the unparticle propagator (see Appendix C) and uses a fixed Z decay width $\Gamma_Z = 2.41$ GeV which is the SM best-fit value for the data. Initial-state QED corrections are also included (see Appendix D).

The allowed regions in the c_V - c_A plane for different values of d and μ are shown in Fig. 5. The best-fit parameters and χ^2 values are listed in Table 2, and fits to FBA data with and without unparticles are displayed in Fig. 6. For values of d close to 1 where fermion-unparticle couplings are less suppressed by M_Z^{1-d} , constraints on c_V and c_A are more stringent and the dependence on μ is more significant. The mono-photon bound discussed in Section 2 is stronger than the muon pair production bound for $d \gtrsim 1.3$.⁶

Finally, it is worth emphasizing that the spin and scale dimension of the exchanged unparticle can be probed by analyzing the scattering angle and energy distributions of differential cross-sections in a linear collider, for both real emission and virtual exchange processes [2, 4, 15]. Furthermore, for polarized beams the azimuthal dependence of the final state fermion can provide an independent measure of the scaling dimension for spin-1 unparticle exchange [33].

⁶Recently, it was noted that processes mediated by unparticle self-interactions lead to multi-body final states which could be the most promising modes for unparticle discovery at colliders [32]. However, details of the hidden sector are required to make predictions.

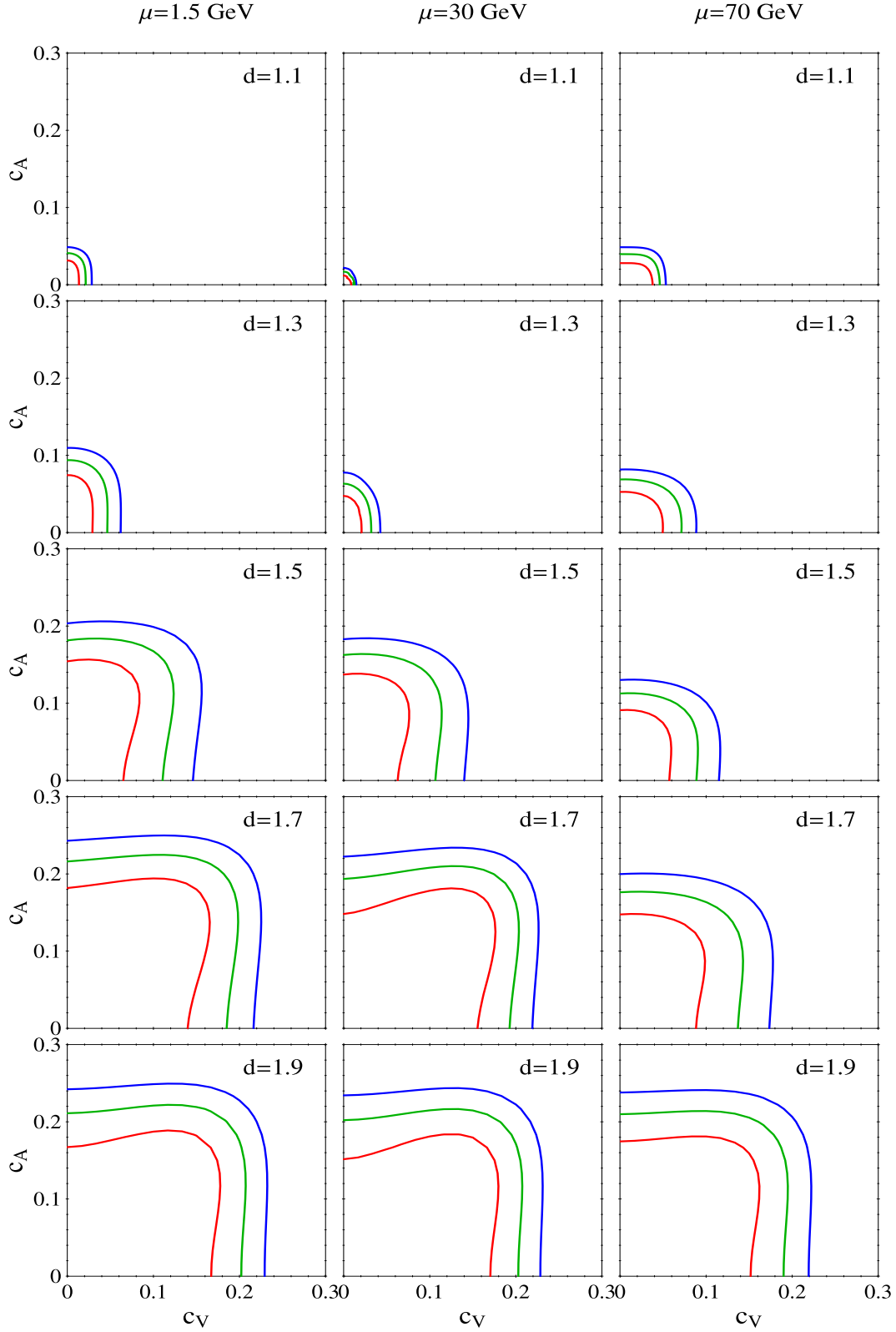


Figure 5: Allowed regions in the c_V - c_A plane from a χ^2 analysis of $e^+e^- \rightarrow \mu^+\mu^-$ cross-section and FBA data. The contours represent the 1σ , 2σ and 3σ regions. We only show results in the first quadrant since the dependence of the cross-section and FBA on the relative sign of c_V and c_A is too weak to be visible.

| d | $\mu = 1.5 \text{ GeV}$ | | | $\mu = 30 \text{ GeV}$ | | | $\mu = 70 \text{ GeV}$ | | |
|-----|-------------------------|--------------------|----------|------------------------|-------|----------|------------------------|--------------------|----------|
| | c_V | c_A | χ^2 | c_V | c_A | χ^2 | c_V | c_A | χ^2 |
| SM | – | – | 154.3 | – | – | 154.3 | – | – | 154.3 |
| 1.1 | 0.001 | 5×10^{-4} | 154.3 | 2×10^{-4} | 0.002 | 154.3 | 0.018 | 4×10^{-4} | 154.0 |
| 1.3 | 0.003 | 0.02 | 154.2 | 1×10^{-4} | 0.02 | 154.2 | 0.0081 | 0.020 | 154.3 |
| 1.5 | 0.0089 | 0.093 | 153.6 | 0.0059 | 0.081 | 153.6 | 0.0016 | 0.036 | 154.2 |
| 1.7 | 0.083 | 0.13 | 153.1 | 0.12 | 0.12 | 152.0 | 0.0071 | 0.081 | 153.9 |
| 1.9 | 0.11 | 0.11 | 152.6 | 0.12 | 0.11 | 152.1 | 0.085 | 0.11 | 153.4 |

Table 2: Best-fit parameters and χ^2 values from an analysis of LEP1-Aleph, KEK-Venus and PETRA-MarkJ $e^+e^- \rightarrow \mu^+\mu^-$ cross-section and FBA data. The dataset is comprised of 55 FBA data points and 54 cross-section data points. The χ^2 value for SM is obtained from a scan on 4 SM parameters M_Z , Γ_Z , e and $\sin\theta_W$. The χ^2 values for SM + unparticles are obtained from a scan on 2 unparticle parameters c_V and c_A for different fixed values of d and μ , with SM parameters fixed to their SM best-fit values.

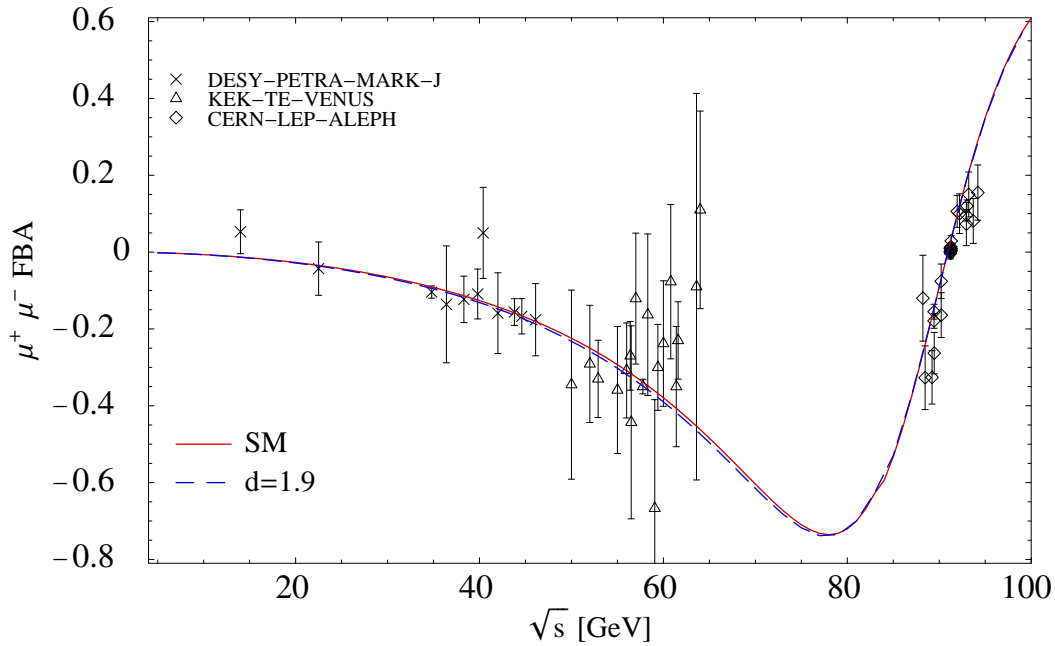


Figure 6: Fits to $e^+e^- \rightarrow \mu^+\mu^-$ FBA data, from a scan over c_V and c_A for different fixed d and μ values. The solid curve (red) is the SM fit and the dashed curve (blue) is the best-fit curve for $d = 1.9$ and $\mu = 1.5 \text{ GeV}$, $\mu = 30 \text{ GeV}$ or $\mu = 70 \text{ GeV}$. For $d \lesssim 1.5$ the curves with unparticle contribution are almost indistinguishable from the SM curve. Note that the unparticle FBA curve does not exhibit divergent behavior at μ as the vacuum polarization introduces a finite decay width and stabilizes the unparticle propagator.

5. Summary

For exact scale invariance, astrophysical and cosmological constraints are in gross conflict with the possibility of probing unparticles in colliders. We showed that for vector unparticles collider constraints become relevant only if scale invariance is broken at a scale $\mu \gtrsim 1$ GeV. Breaking the scale invariance also affects collider expectations by giving rise to a resonance-like behaviour. On the other hand, unparticle effects cannot be observed at energies below the scale μ . We focused on the case $1 \text{ GeV} \lesssim \mu < M_Z$ which allows unparticle effects to show up in Z exchange observables, and gave demonstrations of how this can be realized through unparticle–Higgs couplings.

Simple bounds on vector unparticles have been obtained using effective contact interactions in Refs. [4, 9]. Here we have made a more detailed analysis using $e^+e^- \rightarrow \mu^+\mu^-$ cross-section and forward-backward asymmetry data both at the Z pole and away from it, also taking into account the resonance-like behaviour associated with broken scale invariance. We found that unparticle parameters are severely constrained for values of scale dimension d close to 1. For $d \gtrsim 1.3$, constraints from mono-photon production are more stringent compared to constraints from muon pair production.

Acknowledgments

This research was supported by the U.S. Department of Energy (Grant Nos. DEFG02-95ER40896, DE-FG02-84ER40173 and DE-FG02-04ER41308), by the U.S. National Science Foundation (Grant No. PHY-0544278), and by the Wisconsin Alumni Research Foundation.

A. Unparticle contribution to the Z hadronic width

Ref. [34] studied the real and virtual massive vector boson contribution to the Z hadronic width R_Z . To calculate the constraint on unparticles, we write the unparticle operator in terms of deconstructed particle fields [35]: $O^\mu = \sum_j F_j \lambda_j^\mu$, where the field λ_j^μ has mass $M_j^2 = j\Delta^2$ and

$$F_j^2 = \frac{A_d}{2\pi} \Delta^2 (M_j^2)^{d-2}. \quad (\text{A.1})$$

In the limit $\Delta \rightarrow 0$, the contribution to R_Z is obtained by integrating the contribution from a vector boson with mass m over $\delta = m^2/M_Z^2$:

$$\frac{\Delta R_Z}{R_Z} = \frac{A_d c_V^2}{16\pi^3} \left[\int_0^1 \delta^{d-2} F_1(\delta) d\delta + \int_0^\infty \delta^{d-2} F_2(\delta) d\delta \right], \quad (\text{A.2})$$

where [34]

$$F_1(\delta) = (1 + \delta)^2 [3 \ln \delta + (\ln \delta)^2] + 5(1 - \delta^2) - 2\delta \ln \delta \\ - 2(1 + \delta)^2 \left[\ln(1 + \delta) \ln \delta + \text{Li}_2 \left(\frac{1}{1 + \delta} \right) - \text{Li}_2 \left(\frac{\delta}{1 + \delta} \right) \right], \quad (\text{A.3})$$

$$F_2(\delta) = -2 \left\{ \frac{7}{4} + \delta + \left(\delta + \frac{3}{2}\right) \ln \delta + (1 + \delta)^2 \left[\text{Li}_2 \left(\frac{\delta}{1 + \delta} \right) + \frac{1}{2} \ln^2 \left(\frac{\delta}{1 + \delta} \right) - \frac{\pi^2}{6} \right] \right\}, \quad (\text{A.4})$$

$\text{Li}_2(x) = -\int_0^x dt \ln(1-t)/t$ is the Spence function, and uniform coupling for quarks is assumed. Note that the upper limit 1 of the δ integration is kinematic for the real emission, and the upper limit becomes ∞ for the virtual correction.

Evaluating the integrals, we obtain $\Delta R_Z/R_Z \simeq 0.01c_V^2$, corresponding to a bound $c_V \lesssim 0.3$ since $\Delta R_Z/R_Z = \Delta\alpha_s/\pi \simeq 0.001$. Including the axial-vector coupling is straightforward and leads to $c \lesssim 0.3/\sqrt{2}$.

B. The bound from SN 1987A cooling

As discussed in Refs. [5, 6, 17, 18, 36], SN 1987A energy-loss arguments provide very restrictive constraints on unparticle couplings. In this section we discuss the constraint from pair annihilation of neutrinos and obtain the prefactor C_d in Eqs. (2.8, 3.3) following the method in Refs. [35, 36].⁷

The observed duration of SN 1987A neutrino burst puts a constraint on the supernova volume emissivity [37]

$$Q \lesssim 3 \times 10^{33} \text{ erg cm}^{-3} \text{ s}^{-1}, \quad (\text{B.1})$$

where the supernova core temperature is taken to be $T_{SN} = 30 \text{ MeV}$. This corresponds to

$$Q \lesssim 4 \times 10^{-22} T_{SN}^5. \quad (\text{B.2})$$

As in Appendix A, we write the unparticle operator in terms of deconstructed particle fields. The cross-section for neutrino pair annihilation to λ_j^μ is

$$\sigma_j = \left(\frac{c}{M_Z^{d-1}} \right)^2 A_d \Delta^2 (M_j^2)^{d-2} \delta(s - M_j^2). \quad (\text{B.3})$$

The supernova volume emissivity is found by thermally averaging over the Fermi-Dirac distribution (see e.g. Ref. [38]):

$$Q_j = \int \frac{d^3\mathbf{k}_1}{(2\pi)^3 2E_1} \frac{2}{e^{E_1/T} + 1} \int \frac{d^3\mathbf{k}_2}{(2\pi)^3 2E_2} \frac{2}{e^{E_2/T} + 1} (E_1 + E_2) 2s \sigma_j, \quad (\text{B.4})$$

where we ignored chemical potentials (see Ref. [17]), and $s = 2E_1 E_2 (1 - \cos \theta)$. The total emissivity is obtained as⁸

$$Q = \frac{1}{\Delta^2} \int dM_j^2 Q_j = C_d \left(\frac{c}{M_Z^{d-1}} \right)^2 T_{SN}^{2d+3}, \quad (\text{B.5})$$

⁷The constraint from pair annihilation (for exact scale invariance) is discussed in Ref. [17]. The constraint from nucleon bremsstrahlung is similar in magnitude [5, 6, 17].

⁸See Ref. [36] for similar calculations with tensor unparticles.

where

$$C_d = \frac{2^{2d-3} A_d}{\pi^4 d} \int_0^\infty dx_1 dx_2 \frac{(x_1 x_2)^d (x_1 + x_2)}{(e^{x_1} + 1)(e^{x_2} + 1)} \simeq 0.01. \quad (\text{B.6})$$

We now repeat the calculation for non-zero μ . By matching to the spectral density in Eq. (3.1), we have

$$F_j^2 = \frac{A_d}{2\pi} \Delta^2 (M_j^2 - \mu^2)^{d-2} \theta(M_j^2 - \mu^2), \quad (\text{B.7})$$

$$\sigma_j = \left(\frac{c}{M_Z^{d-1}} \right)^2 A_d \Delta^2 (M_j^2 - \mu^2)^{d-2} \theta(M_j^2 - \mu^2) \delta(s - M_j^2). \quad (\text{B.8})$$

Using Eqs. (B.4, B.8), we obtain Eq. (B.5) with

$$C_d = \frac{2^{d-3} A_d}{\pi^4} \int_0^\infty dx_1 \int_{\mu^2/(4T_{SN}^2 x_1)}^\infty dx_2 \int_{-1}^{1-\mu^2/(2T_{SN}^2 x_1 x_2)} d(\cos \theta) \frac{(x_1 x_2)^d (x_1 + x_2) (1 - \cos \theta) \left(1 - \cos \theta - \frac{\mu^2}{2T_{SN}^2 x_1 x_2} \right)^{d-2}}{(e^{x_1} + 1)(e^{x_2} + 1)}. \quad (\text{B.9})$$

The approximation Eq. (3.3) is obtained from Eq. (B.9) assuming $\mu \gg T_{SN}$.

C. Vacuum polarization correction

To lowest order, $\Pi(q^2)$ in Eq. (4.1) is given as follows:

$$\Pi = \Pi_{LL} + \Pi_{LR} + \Pi_{RL} + \Pi_{RR}, \quad (\text{C.1})$$

$$\Pi_{LR} = \Pi_{RL} = -2 \frac{c_L c_R}{16\pi^2 M_Z^{2d-2}} \int_0^1 dx m_f^2 \log \left(\frac{m_f^2}{m_f^2 - x(1-x)q^2} \right), \quad (\text{C.2})$$

$$\Pi_{LL/RR} = -4 \frac{c_{L/R} c_{L/R}}{16\pi^2 M_Z^{2d-2}} \int_0^1 dx \left(x(1-x)q^2 - \frac{1}{2} m_f^2 \right) \log \left(\frac{m_f^2}{m_f^2 - x(1-x)q^2} \right), \quad (\text{C.3})$$

where $c_L = c_V - c_A$, $c_R = c_V + c_A$ and m_f is the mass of the fermion in the loop. $\Pi(q^2)$ is complex for the s channel with $q^2 > 4m_f^2$, and the imaginary part will stabilize the propagator when the real part coincides with the pole. We assume a universal coupling between the unparticle and different fermions that include charged leptons, neutrinos and quarks. A numerical example for $\Pi(q^2)$ that is summed over the fermions is shown in Fig. 7.

D. Initial state QED corrections

Initial state QED corrections significantly affect the cross-section and FBA around μ (see Fig. 8). Since the corrections to the SM cross-section σ_{SM} are removed from the KEK-Venus and PETRA-MarkJ data, we only consider the corrections to the unparticle exchange

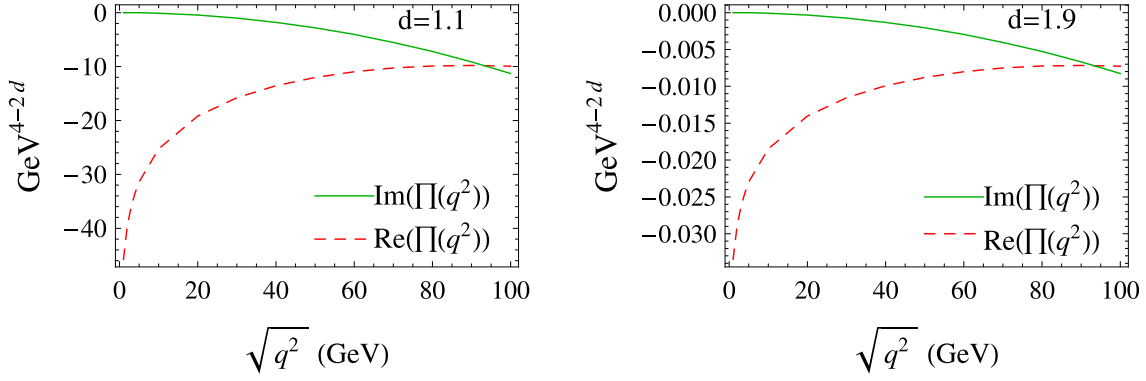


Figure 7: $\Pi(q^2)$ from charged lepton, neutrino and quark loops, assuming fermion couplings $c_V = c_A = 0.05$.

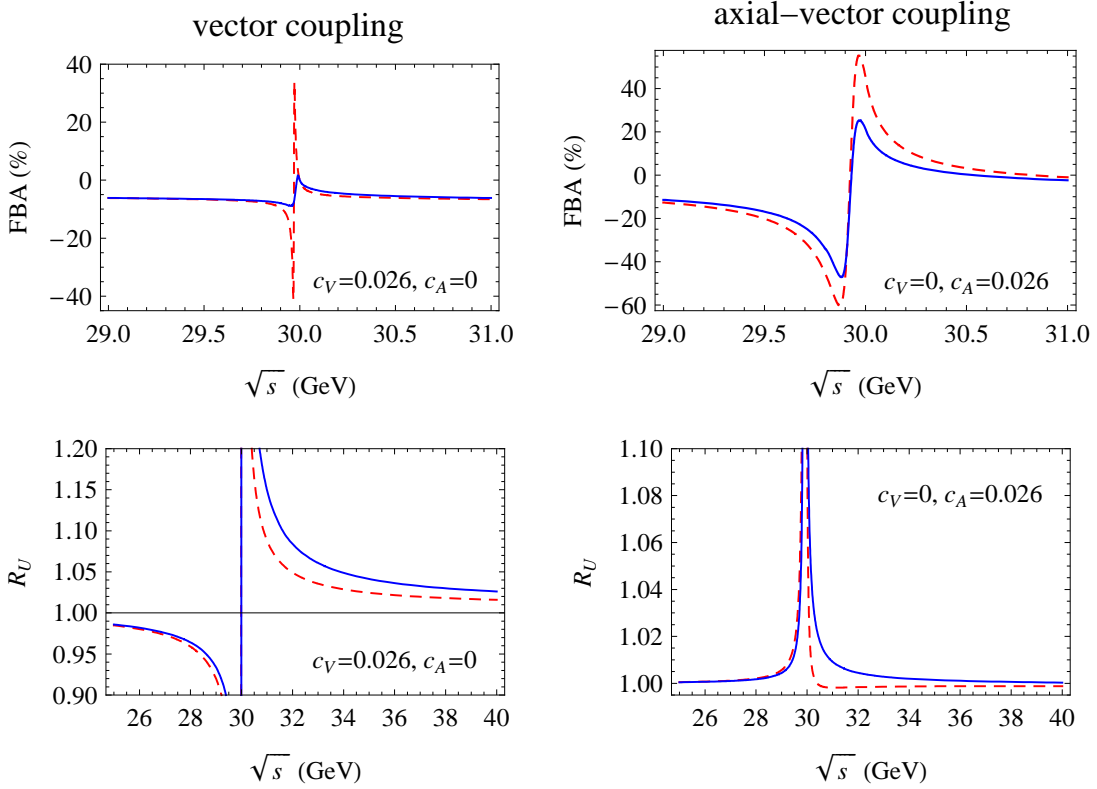


Figure 8: FBA and R_U for $e^+e^- \rightarrow \mu^+\mu^-$, $d = 1.1$ and $\mu = 30$ GeV. Solid blue curves: with initial state QED corrections to the unparticle exchange term as well as the interference terms between γ, Z and the unparticle. Red dashed curves: without initial state QED corrections. ($c_{V,A} = 0.026$ correspond to the mono-photon bound of section 2.)

term σ_U and the interference terms σ_{int} between γ, Z and the unparticle. The corrected cross section is obtained by convoluting the relevant terms with a radiator function $H(x)$:

$$\sigma(s) = \sigma_{SM}(s) + \int_0^{1-4m_\mu^2/s} dx H(x) (\sigma_U[s(1-x)] + \sigma_{\text{int}}[s(1-x)]), \quad (\text{D.1})$$

where [39]

$$H(x) = \beta x^{\beta-1} \delta^V + \delta^h \quad (\text{D.2})$$

with

$$\begin{aligned} \beta &= \frac{2\alpha}{\pi}(L-1), \quad L = \log \frac{s}{m_e^2}, \quad \delta^V = 1 + \frac{\alpha}{\pi} \left(\frac{3}{2}L + \frac{\pi^2}{3} - 2 \right) + \dots, \\ \delta^h &= \frac{\alpha}{\pi}(L-1)(x-2) + \dots \end{aligned} \quad (\text{D.3})$$

The LEP1-Aleph data are fitted with full QED corrections, since the corrections to σ_{SM} are not removed.

The corrected FBA for KEK-Venus and PETRA-MarkJ data is obtained in a similar manner [40]:

$$\text{FBA}(s) = \frac{1}{\sigma(s)} \left[\sigma_{SM}^{FB}(s) + \int_{4m_\mu^2/s}^1 dz \frac{4z}{(1+z)^2} \tilde{H}(z) (\sigma_U^{FB}(zs) + \sigma_{\text{int}}^{FB}(zs)) \right], \quad (\text{D.4})$$

where

$$\sigma^{FB} = \int_{\theta > \pi/2} d\Omega \frac{d\sigma}{d\Omega} - \int_{\theta < \pi/2} d\Omega \frac{d\sigma}{d\Omega}, \quad (\text{D.5})$$

$$\begin{aligned} \tilde{H}(z) &= H(1-z) + \left(\frac{\alpha}{2\pi} \right)^2 L^2 \left[\frac{(1-z)^3}{2z} - (1+z) \log(z) + 2(1-z) \right. \\ &\quad \left. + \frac{(1-z)^2}{\sqrt{z}} \left(\arctan \frac{1}{\sqrt{z}} - \arctan \sqrt{z} \right) \right]. \end{aligned} \quad (\text{D.6})$$

Again, the LEP1-Aleph data are fitted with full QED corrections.

At the energy scale M_Z with the scaling breaking parameter $\mu \gtrsim 1$ GeV, unparticle bremsstrahlung is not effective and thus not included.

References

- [1] H. Georgi, *Phys. Rev. Lett.* **98** (2007) 221601, [[hep-ph/0703260](#)].
- [2] H. Georgi, *Phys. Lett.* **B650** (2007) 275–278, [[arXiv:0704.2457 \[hep-ph\]](#)].
- [3] K. Cheung, W.-Y. Keung, and T.-C. Yuan, *Phys. Rev. Lett.* **99** (2007) 051803, [[arXiv:0704.2588 \[hep-ph\]](#)].
- [4] K. Cheung, W.-Y. Keung, and T.-C. Yuan, *Phys. Rev.* **D76** (2007) 055003, [[arXiv:0706.3155 \[hep-ph\]](#)].
- [5] H. Davoudiasl, *Phys. Rev. Lett.* **99** (2007) 141301, [[arXiv:0705.3636 \[hep-ph\]](#)].
- [6] A. Freitas and D. Wyler, *JHEP* **12** (2007) 033, [[arXiv:0708.4339 \[hep-ph\]](#)].
- [7] T. G. Rizzo, *JHEP* **10** (2007) 044, [[arXiv:0706.3025 \[hep-ph\]](#)].
- [8] P. J. Fox, A. Rajaraman, and Y. Shirman, *Phys. Rev.* **D76** (2007) 075004, [[arXiv:0705.3092 \[hep-ph\]](#)].
- [9] M. Bander, J. L. Feng, A. Rajaraman, and Y. Shirman, *Phys. Rev.* **D76** (2007) 115002, [[arXiv:0706.2677 \[hep-ph\]](#)].
- [10] M.-x. Luo, W. Wu, and G.-h. Zhu, *Phys. Lett.* **B659** (2008) 349, [[arXiv:0708.0671 \[hep-ph\]](#)].
- [11] B. Grinstein, K. Intriligator and I. Z. Rothstein, [arXiv:0801.1140 \[hep-ph\]](#).
- [12] G. Mack, *Commun. Math. Phys.* **55** (1977) 1.
- [13] Y. Nakayama, *Phys. Rev.* **D76** (2007) 105009, [[arXiv:0707.2451 \[hep-ph\]](#)].
- [14] P. Achard et al. (L3 Collaboration), *Phys. Lett.* **B587** (2004) 16–32, [[hep-ex/0402002](#)].
- [15] S.-L. Chen and X.-G. He, *Phys. Rev.* **D76** (2007) 091702, [[arXiv:0705.3946 \[hep-ph\]](#)].
- [16] M. Acciarri et al. (L3 Collaboration), *Phys. Lett.* **B470** (1999) 281, [[hep-ex/9910056](#)].
- [17] S. Hannestad, G. Raffelt, and Y. Y. Y. Wong, *Phys. Rev.* **D76** (2007) 121701, [[arXiv:0708.1404 \[hep-ph\]](#)].
- [18] P. K. Das, *Phys. Rev.* **D76** (2007) 123012, [[arXiv:0708.2812 \[hep-ph\]](#)]; S. Dutta and A. Goyal, [arXiv:0712.0145 \[hep-ph\]](#).
- [19] J. McDonald, [arXiv:0709.2350 \[hep-ph\]](#).
- [20] N. G. Deshpande, S. D. H. Hsu, and J. Jiang, [arXiv:0708.2735 \[hep-ph\]](#).
- [21] Y. Liao, *Phys. Rev.* **D76** (2007) 056006, [[arXiv:0705.0837 \[hep-ph\]](#)].
- [22] L. Anchordoqui and H. Goldberg, *Phys. Lett.* **B659** (2008) 345, [[arXiv:0709.0678 \[hep-ph\]](#)].
- [23] A. B. Balantekin and K. O. Ozansoy, *Phys. Rev.* **D76** (2007) 095014, [[arXiv:0710.0028 \[hep-ph\]](#)].
- [24] D. Choudhury, D. K. Ghosh, and Mamta, *Phys. Lett.* **B658** (2008) 148, [[arXiv:0705.3637 \[hep-ph\]](#)]; S. Zhou, *Phys. Lett.* **B659** (2008) 336, [[arXiv:0706.0302 \[hep-ph\]](#)].
- [25] R. Zwicky, [arXiv:0707.0677 \[hep-ph\]](#).
- [26] T. Kikuchi and N. Okada, [arXiv:0707.0893 \[hep-ph\]](#).

- [27] A. Delgado, J. R. Espinosa, and M. Quiros, *JHEP* **10** (2007) 094, [[arXiv:0707.4309](#) [[hep-ph](#)]].
- [28] N. G. Deshpande, X.-G. He, and J. Jiang, *Phys. Lett.* **B656** (2007) 91–95, [[arXiv:0707.2959](#) [[hep-ph](#)]].
- [29] J. Kile and M. J. Ramsey-Musolf, *Phys. Rev.* **D76** (2007) 054009, [[arXiv:0705.0554](#) [[hep-ph](#)]].
- [30] B. Adeva et al. (MARK J Collaboration), *Phys. Rev.* **D38** (1988) 2665; *Phys. Rev. Lett.* **55** (1985) 665.
- [31] R. Barate et al. (ALEPH Collaboration), *Eur. Phys. J.* **C14** (2000) 1–50; M. Miura et al. (VENUS Collaboration), *Phys. Rev.* **D57** (1998) 5345–5362; K. Abe et al. (VENUS Collaboration), *Z. Phys.* **C48** (1990) 13; *Phys. Lett.* **B246** (1990) 297.
- [32] M. J. Strassler, [arXiv:0801.0629](#) [[hep-ph](#)]; J. L. Feng, A. Rajaraman and H. Tu, [arXiv:0801.1534](#) [[hep-ph](#)].
- [33] K. Huitu and S. K. Rai, [arXiv:0711.4754](#) [[hep-ph](#)].
- [34] C. D. Carone and H. Murayama, *Phys. Rev. Lett.* **74** (1995) 3122, [[hep-ph/9411256](#)].
- [35] M. A. Stephanov, *Phys. Rev.* **D76** (2007) 035008, [[arXiv:0705.3049](#) [[hep-ph](#)]].
- [36] I. Lewis, [arXiv:0710.4147](#) [[hep-ph](#)].
- [37] G. G. Raffelt, *Phys. Rept.* **198** (1990) 1–113.
- [38] J. Goodman, A. Dar, and S. Nussinov, *Astrophys. J.* **314** (1987) L7–L10.
- [39] F. A. Berends, W. L. van Neerven and G. J. H. Burgers, *Nucl. Phys.* **B297** (1988) 429 [Erratum-ibid. **B304** (1988) 921]. For a review and references, see W. Hollik and G. Duckeck, *Springer Tracts Mod. Phys.* **162** (2000) 1.
- [40] D. Y. Bardin et al., *Phys. Lett.* **B229** (1989) 405; D. Y. Bardin et al., *Nucl. Phys.* **B351** (1991) 1, [[hep-ph/9801208](#)]; W. Beenakker, F. A. Berends and S. C. van der Marck, *Phys. Lett.* **B251** (1990) 299.